A note on the relationship between dip-slip fault parameters and plate parameters in the two-dimensional modelling of preseismic deformation

SARVA JIT SINGH and MAHABIR SINGH

Department of Mathematics, Maharshi Dayanand University, Rohtak 124 001, India

Preseismic lithospheric deformation at a subduction zone can be modelled as dip-slip dislocation on an inclined fault or as flexure of a thin plate. Both these models predict a region of positive topography known as forebulge or outer rise. By matching the location and the magnitude of the forebulge, we derive useful relations between the dip-slip fault parameters and the plate parameters. In particular, we determine the width of a long dip-slip fault of given dip corresponding to a semi-infinite plate of given thickness. The displacement profiles of the two models are also compared.

1. Introduction

Two-dimensional dip-slip dislocation models have been used extensively to model the lithospheric deformation associated with thrust faulting at subduction zones (see, e.g., Cohen 1992 and the references listed therein). Rani and Singh (1992) and Singh and Rani (1993) studied in great detail the deformation of a uniform half-space by a two-dimensional dip-slip fault. Cohen (1996) gave convenient formulas for determining dip-slip fault parameters from geophysical observables.

Hastie and Savage (1970), amongst others, presented a dislocation model for the 1964 Alaska earthquake. In contrast, Rosenbaum (1974) used plate flexure theory to model the warping of southern Alaska before the 1964 Alaska earthquake. By assuming complete elastic rebound during the earthquake, Rosenbaum (1974) showed that the calculated displacements are compatible with the observed pre-earthquake deformation. In dislocation theory, the entire half-space below the Earth's surface is treated as a semi-infinite homogeneous elastic body, and surface displacements are modelled as a result of movement on an inclined fault plane. Plate flexure theory provides an alternative approach to dislocation theory, working in terms of effects of forces acting on the plate. Two-dimensional thin-plate theory has been widely used to model lithospheric deformation associated with dip-slip faulting (see, e.g., Caldwell *et al* 1976; Parsons and Molnar 1976; Chapple and Forsyth 1979; Turcotte 1979; Turcotte and Schubert 1982; Savage and Gu 1985; Bott 1996).

2. Dip-slip fault

For a surface-breaking thrust fault of finite width, L, and infinite length embedded in a uniform elastic half-space, the surface uplift of the hanging wall is given by (Savage 1980; Singh and Rani 1993)

$$v = \frac{b}{\pi}\sin\delta\left[\frac{\pi}{2} - \tan^{-1}\left(\frac{X_1 - \cos\delta}{\sin\delta}\right) - \frac{X_1\sin\delta}{X_1^2 - 2X_1\cos\delta + 1}\right], \quad (1)$$

where $X_1 = x/L > 0$, b is the magnitude of dislocation (slip) and δ is the dip angle ($0 \le \delta \le \pi/2$). As shown in figure 1, the origin is taken at the outcrop of the fault plane, x-axis in the dip-direction and y-axis vertically upwards. The key parameters that determine the shape of the displacement profile are the

Keywords. Dip-slip faulting; plate flexure; preseismic deformation; subduction zone.

Proc. Indian Acad. Sci. (Earth Planet. Sci.), **107**, No. 2, June 1998, pp. 155–160

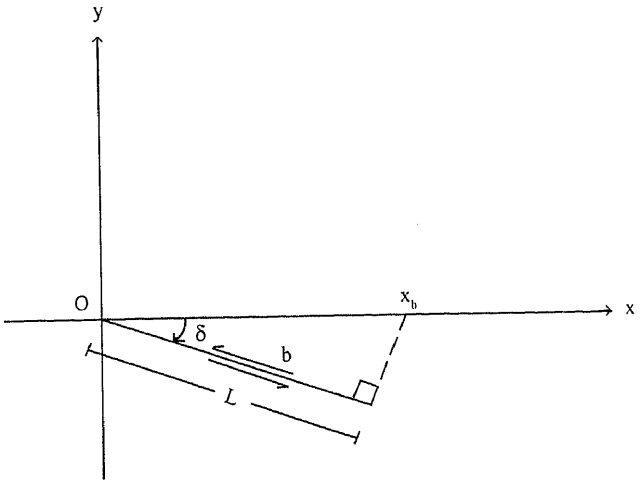

Figure 1. Geometry of a two-dimensional dip-slip fault of width L and dip δ. b denotes the slip.

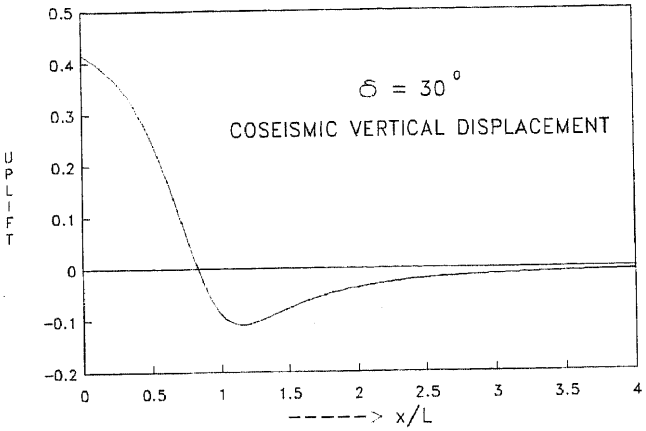

Figure 2. Variation of the vertical (up) displacement due to a thrust fault with the distance from the fault for $\delta = 30°$. The displacement is measured in units of the slip b.

fault width, L, and the dip angle, δ. The surface displacements due to a dip-slip fault in a uniform half-space are independent of the elastic parameters of the medium.

The maximum uplift occurs at the origin, with the value

$$v_0 = \left(1 - \frac{\delta}{\pi}\right) b \sin\delta.$$

As shown by Singh and Rani (1993), the subsidence $(-v)$ is maximum at $x = x_b = L/\cos\delta$, and the maximum value is given by

$$-v_b = \frac{b}{\pi}\left[\cos\delta - \left(\frac{\pi}{2} - \delta\right)\sin\delta\right], \tag{2}$$

which is a decreasing function of δ. Note that both v_0 and v_b are independent of L.

Figure 2 shows the variation of the uplift with the distance from the fault for $\delta = 30°$. In this case, $v_0 = 0.42b$, $v_b = -0.11b$, $x_b = 1.15L$. Moreover, $v = 0$ at $x = 0.82L$. The displacement profile of figure 3 is

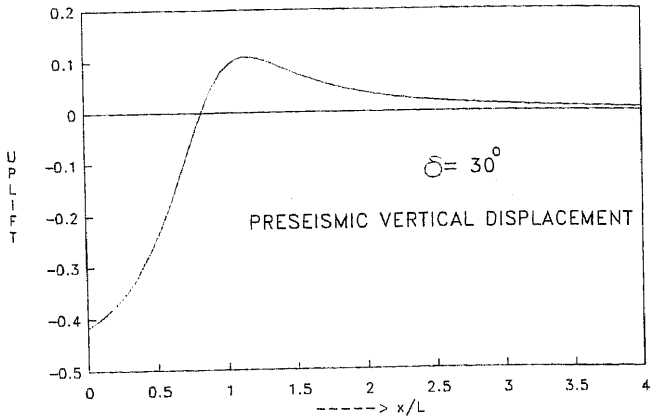

Figure 3. Profile of figure 2 reflected about the x-axis. Assuming complete elastic rebound during an earthquake, if figure 2 represents coseismic vertical displacement, then figure 3 represents preseismic vertical displacement.

merely the displacement profile of figure 2 reflected about the x-axis. On the assumption that complete elastic rebound occurs at the time of an earthquake, if figure 2 represents coseismic displacement profile, then figure 3 represents preseismic displacement profile corresponding to the preearthquake strain accumulation (Rosenbaum 1974). Since the displacement profile of figure 3 is similar to the shape of a thin elastic plate deformed by an end load, we examine the resemblance minutely and derive useful relations between the dip-slip fault parameters and the plate parameters.

3. Two-dimensional flexure of a thin plate

The analysis of this section follows closely the treatment of Turcotte and Schubert (1982).

The thin elastic surface plates constitute the elastic lithosphere, which floats on a relatively fluid substratum. We consider two-dimensional bending of a thin elastic semi-infinite plate floating on a fluid half-space and subjected to end loading. The plate is terminated at one end by the fault and extends infinitely in the other direction. Taking x-axis in the horizontal direction and y-axis vertically upwards (figure 4), the vertical deflection, v, of the plate is governed by the equation

$$D\frac{d^4v}{dx^4} + \rho g v = 0, \tag{3}$$

where D is the flexural rigidity,

$$D = \frac{Eh^3}{12(1-\nu^2)} \tag{4}$$

and

g acceleration of gravity,

E Young's modulus of the plate,

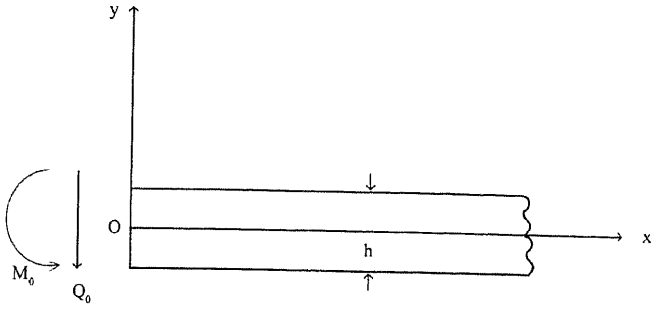

Figure 4. Geometry of a semi-infinite plate of thickness h under end loading, which is either a shear force Q_0 or a bending moment M_0. The plate is terminated at the origin by the fault and extends to infinity in the positive x-direction.

ν Poisson's ratio of the plate,

h thickness of the plate,

ρ density of the fluid substratum.

The bending moment, M, and the shear force, Q, at any cross-section of the plate are given by

$$M = -D\frac{d^2v}{dx^2}, Q = -D\frac{d^3v}{dx^3}. \tag{5}$$

A suitable solution of equation (3) is of the form

$$v = [a_1 \cos(x/\alpha) + a_2 \sin(x/\alpha)]e^{-x/\alpha}, \quad (x \geq 0), \tag{6}$$

where

$$\alpha = (4D/\rho g)^{1/4} \tag{7}$$

is the flexural parameter. In general, the free end of the plate will be under the action of a bending moment and a shear line load. However, for the sake of clarity, we consider the bending moment loading and the shear loading separately.

3.1 *Shear load*

We apply the boundary condition that the bending moment, M, vanishes at the free end, so that

$$\frac{d^2v}{dx^2} = 0 \text{ at } x = 0. \tag{8}$$

From equations (6) and (8), we get $a_2 = 0$, so that

$$v = v_0 \cos X e^{-X}, \tag{9}$$

where $X = x/\alpha$ and v_0 is the deflection of the free end. The deflection is maximum at $x = x_b = (3\pi/4)\alpha$ and the maximum deflection is

$$v_b = -\frac{v_0}{\sqrt{2}} e^{-3\pi/4} = -0.067 v_0. \tag{10}$$

The shear load at the end $x = 0$ causing the deflection is given by

$$Q_0 = -D\left(\frac{d^3v}{dx^3}\right)_0 = -2v_0 D/\alpha^3. \tag{11}$$

3.2 *Bending moment*

The boundary condition that the shear load vanishes at the free end implies

$$\frac{d^3v}{dx^3} = 0 \text{ at } x = 0. \tag{12}$$

Equations (6) and (12) yield $a_2 = -a_1$ so that

$$v = v_0 \quad \sqrt{2}\cos(X + \pi/4)e^{-X}. \tag{13}$$

The maximum deflection occurs at $x = x_b = (\pi/2)\alpha$ and

$$v_b = -v_0 e^{-\pi/2} = -0.207 v_0. \tag{14}$$

The bending moment at the end $x = 0$ is

$$M_0 = -D\left(\frac{d^2v}{dx^2}\right)_0 = -2v_0 D/\alpha^2.$$

4. Relationship between the dip-slip fault parameters and the plate parameters

The shape of the displacement profile given by equation (1) is determined by two fault parameters: fault width, L, and fault dip, δ. The shape of the deflection profile is determined by the flexural parameter, α. We establish useful relations between these parameters by matching conspicuous features of the two profiles. We consider the two cases of deflection of a thin plate by end loading consisting of a shear line load and bending moment separately. It may be emphasized that in the following we are going to compare the dip-slip fault model of the preseismic deformation (changing v to $-v$ in equation (1)) with the plate model.

4.1 *Shear load*

If we assume that the point of maximum uplift of the fault model coincides with the point of maximum positive deflection, we get

$$\frac{L}{\cos\delta} = \frac{3\pi}{4}\alpha,$$

i.e.

$$L = L_F = \frac{3\pi}{4}\alpha\cos\delta, \tag{15}$$

where the subscript F indicates that the value is for a shear load (force). Putting the value of the flexural parameter from equations (4) and (7), we get

$$L_F = \frac{3\pi}{4}\cos\delta\left[\frac{E}{3(1-\nu^2)g\rho}\right]^{1/4} h^{3/4}. \tag{16}$$

We assume the following numerical values for various parameters appearing in the expression for L_F (Savage and Gu 1985)

$\nu = 0.25$,

$g = 9.8\,\mathrm{m\,s^{-2}}$,

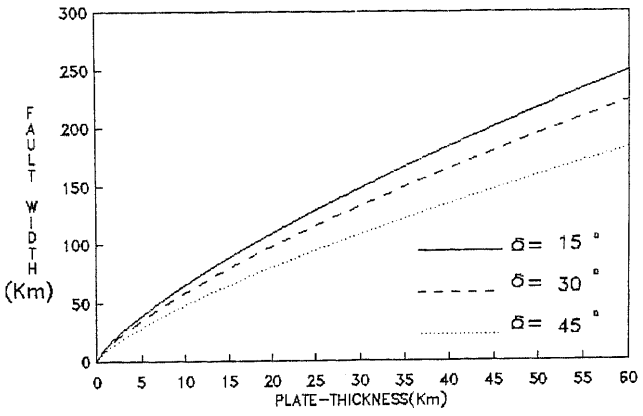

Figure 5. Fault-width for the two-dimensional dip-slip fault model for $\delta = 15°, 30°, 45°$ corresponding to the plate model of a given thickness with line shear force end loading.

$$\rho = 3800\,\mathrm{kg\,m^{-3}},$$
$$E = 70\,\mathrm{G\,Pa}.$$

Figure 5 gives the value of the fault width of the dip-slip fault model for a given value of the plate thickness for three values of the dip angle $\delta = 15°, 30°, 45°$.

Next, equating the maximum uplift of the fault model (equation (2) with sign changed) with the maximum positive deflection (equation (10)), we obtain

$$v_0 = -\frac{b\sqrt{2}}{\pi}\left[\cos\delta - \left(\frac{\pi}{2} - \delta\right)\sin\delta\right] e^{3\pi/4}. \tag{17}$$

From equations (10), (11) and (17), we have

$$v = -\frac{b\sqrt{2}}{\pi}\left[\cos\delta - \left(\frac{\pi}{2} - \delta\right)\sin\delta\right] e^{3\pi/4}\cos X e^{-X}, \tag{18}$$

$$Q_0 = \frac{2\sqrt{2}}{\pi} b\left(\frac{D}{\alpha^3}\right)\left[\cos\delta - \left(\frac{\pi}{2} - \delta\right)\sin\delta\right] e^{3\pi/4}. \tag{19}$$

Figure 6(a) shows the variation of the dimensionless deflection (v/b) for the plate model with the dimensionless distance $X = x/\alpha$ for $\delta = 15°$. The displacement profile for the fault model is also shown which is calculated from equation (1), with sign reversed, using the relation

$$X_1 = x/L = \left(\frac{4}{3\pi\cos\delta}\right) X,$$

which follows from equation (15). Figure 6(b and c) are for $\delta = 30°$ and $60°$, respectively.

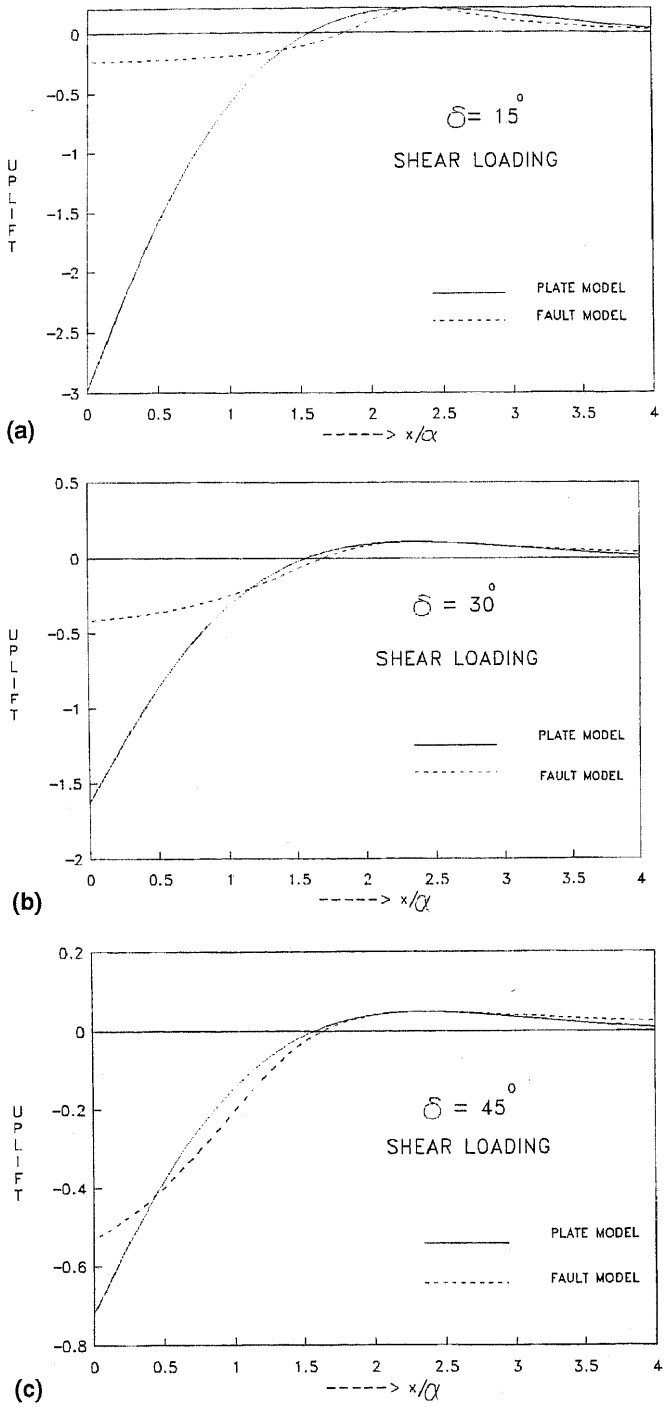

Figure 6(a, b and c). Variation of the vertical (up) displacement with distance for the dip-slip fault model and the plate model with shear loading for (**a**) $\delta = 15°$; (**b**) $\delta = 30°$; (**c**) $\delta = 45°$. The displacement is measured in units of the slip b of the fault model.

4.2 *Bending moment*

If we assume that the point of maximum uplift of the fault model coincides with the point of maximum positive deflection of the plate model with bending moment end loading, we get

$$\frac{L}{\cos\delta} = \frac{\pi}{2}\alpha,$$

i.e.

$$L = L_M = \frac{\pi}{2}\alpha\cos\delta = \frac{2}{3}L_F, \tag{20}$$

where the subscript M indicates bending moment loading and L_F is given by equation (16).

As before, equating the maximum uplift of the fault model with the maximum positive deflection

(equation (14)), we get

$$v_0 = -\frac{b}{\pi}\left[\cos\delta - \left(\frac{\pi}{2} - \delta\right)\sin\delta\right] e^{\pi/2}, \tag{21}$$

so that

$$v = -b\frac{\sqrt{2}}{\pi}\left[\cos\delta - \left(\frac{\pi}{2} - \delta\right)\sin\delta\right] e^{3\pi/4} \times \cos\left(X + \frac{\pi}{4}\right) e^{-(X+\pi/4)}, \tag{22}$$

$$M_0 = \frac{2}{\pi} b \left(\frac{D}{\alpha^2}\right)\left[\cos\delta - \left(\frac{\pi}{2} - \delta\right)\sin\delta\right] e^{\pi/2}. \tag{23}$$

In the present case,

$$X_1 = x/L = \left(\frac{2}{\pi\cos\delta}\right) X,$$

using equation (20).

Figure 7(a) shows the deflection of a thin plate with bending moment end loading as well as the variation of the displacement due to a fault model with x/α for $\delta = 15°$. Figures 7(b) and (c) are for $\delta = 30°$ and 45°, respectively.

5. Discussion

We have considered two models of the vertical deformation due to preseismic stressing, namely, dislocation and plate flexure. Both models predict subsidence in the near field and uplift at greater distances from the fault. By setting equal the location of the maximum uplift predicted by the two models, we have found a relationship between the fault width in the dislocation model and the elastic plate thickness parameter in the flexure model. Two options are investigated in the flexure model: in one case the bending moment at the end of the plate vanishes and in the other case the shear load vanishes. We also equate the amplitudes of the maximum uplift predicted by the two models. This enables us to derive further relationships between the models. The results are potentially very important because they would allow for an estimation of the plate thickness from geodetic or seismic observations or estimates of fault properties from non-seismic data.

Equation (16) gives the width of a two-dimensional dip-slip fault of a given dip corresponding to a semi-infinite plate of a given thickness with shear line load at the free end. We note that L_F is a decreasing function of δ. Equation (19) can be used to estimate the shear end load corresponding to a given dip and slip. Equation (20) shows that the fault width corresponding to the bending moment loading is two-thirds of the fault width corresponding to the shear end loading.

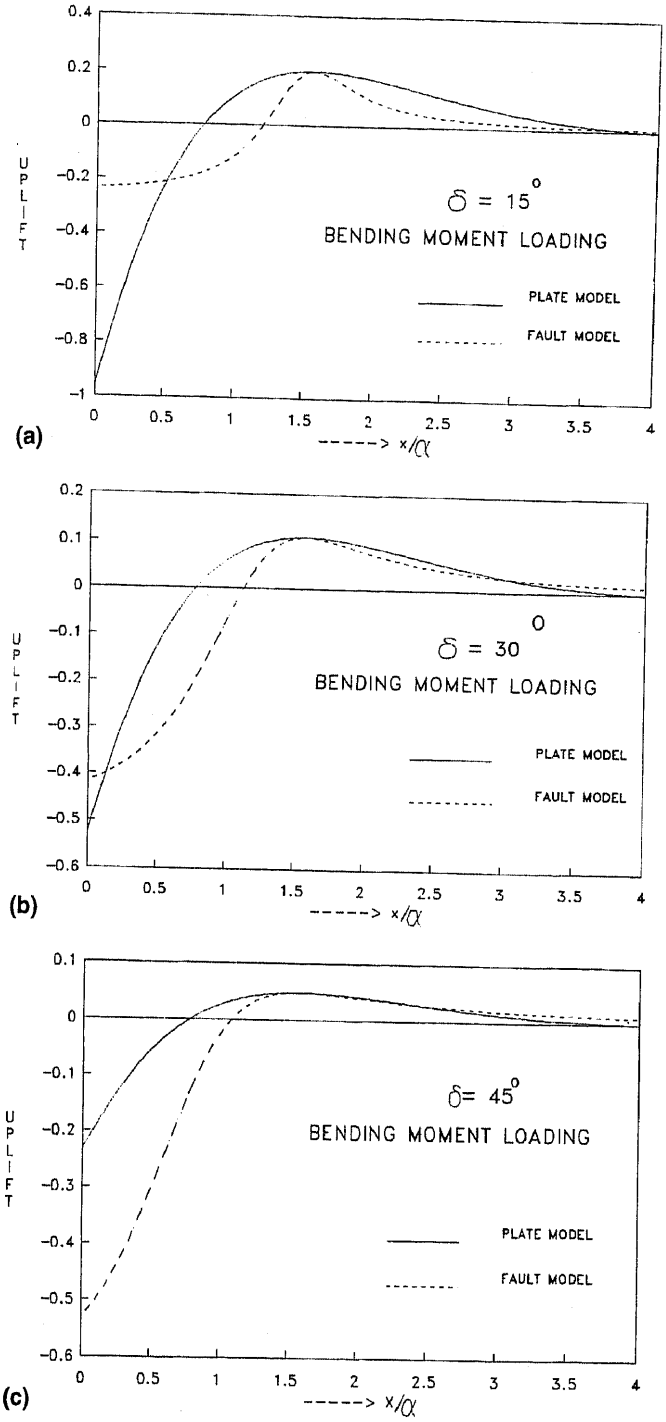

Figure 7(a, b and c). Variation of the vertical (up) displacement with distance for the dip-slip fault model and the plate model with bending moment loading for (**a**) $\delta = 15°$; (**b**) $\delta = 30°$; (**c**) $\delta = 45°$. The displacement is measured in units of the slip b of the fault model.

References

Bott M H P 1996 Flexure associated with planar faulting: *Geophys. J. Int.* **126** F21–F24

Caldwell J G, Haxby D E, Karig D E and Turcotte D L 1976 On the applicability of a universal elastic trench profile; *Earth Planet. Sci. Lett.* **31** 239–246

Chapple W M and Forsyth D W 1979 Earthquakes and bending of plates and trenches; *J. Geophys. Res.* **84** 6729–6749

Cohen S C 1992 Postseismic deformation and stress diffusion due to viscoelasticity and comments on the modified Elasser model; *J. Geophys. Res.* **97** 15395–15403

Cohen S C 1996 Convenient formulas for determining dip-slip fault parameters from geophysical observables; *Bull. Seis. Soc. Am.* **86** 1642–1644

Hastie L M and Savage J C 1970 A dislocation model for the 1964 Alaska earthquake; *Bull. Seis. Soc. Am.* **60** 1389–1392

Parsons B and Molnar P 1976 The origin of outer topographic rises associated with trenches; *Geophys. J. R. Astr. Soc.* **45** 707–712

Rani S and Singh S J 1992 Static deformation of a uniform half-space due to a long dip-slip fault; *Geophys. J. Int.* **109** 469–476

Rosenbaum J G 1974 Theory of warping of southern Alaska before Alaska earthquake 1964; *J. Geophys. Res.* **79** 3294–3301

Savage J C 1980 Dislocations in seismology, in *Dislocations in Solids*, Vol. 3, *Moving Dislocations*, (ed) F R N Nabarro North-Holland, Amsterdam pp. 251–339

Savage J C and Gu G 1985 A plate flexure approximation to postseismic and interseismic deformation; *J. Geophys. Res.* **90** 8570–8580

Singh S J and Rani S 1993 Crustal deformation associated with two-dimensional thrust faulting; *J. Phys. Earth* **41** 87–101

Turcotte D L 1979 Flexure, in *Advances in Geophysics* Vol. 21, (New York: Academic Press) pp. 51–86

Turcotte D L and Schubert G 1982 *Geodynamics: Applications of Continuum Physics to Geological Problems*, (New York: John Wiley)

MS received 8 July 1997; revised 12 February 1998